ACS OMEGA

Article

Cite This: ACS Omega 2019, 4, 4029−4039

http://pubs.acs.org/journal/acsodf

Reducing the Amyloidogenicity of Functional Amyloid Protein FapC Increases Its Ability To Inhibit α-Synuclein Fibrillation

Line Friis Bakmann Christensen,[†] Kirstine Friis Jensen,[†] Janni Nielsen,[†] Brian Stougaard Vad,[†] Gunna Christiansen,[‡] and Daniel Erik Otzen*[,†]

[†]Interdisciplinary Nanoscience Center (iNANO), Department of Molecular Biology and Genetics, Aarhus University, Gustav Wieds Vej 14, DK, 8000 Aarhus C, Denmark

[‡]Section for Medical Microbiology and Immunology, Department of Biomedicine, Aarhus University, Vennelyst Boulevard 4, 8000 Aarhus C, Denmark

Supporting Information

ABSTRACT: Functional amyloid (FA) proteins have evolved to assemble into fibrils with a characteristic cross-β structure, which stabilizes biofilms and contributes to bacterial virulence. Some of the most studied bacterial FAs are the curli protein CsgA, expressed in a wide range of bacteria, and FapC, produced mainly by members of the *Pseudomonas* genus. Though unrelated, both CsgA and FapC contain imperfect repeats believed to drive the formation of amyloid fibrils. While much is known about CsgA biogenesis and fibrillation, the mechanism of FapC fibrillation remains less explored. Here, we show that removing the three imperfect repeats of FapC (FapC ΔR1R2R3) slows down the fibrillation but does not prevent it. The increased lag phase seen for FapC ΔR1R2R3 allows for disulfide bond formation, which further delays fibrillation. Remarkably, these disulfide-bonded species of FapC ΔR1R2R3 also significantly delay the fibrillation of human α-synuclein, a key protein in Parkinson's disease pathology. This attenuation of α-synuclein fibrillation was not seen for the reduced form of FapC ΔR1R2R3. The results presented here shed light on the FapC fibrillation mechanism and emphasize how unrelated fibrillation systems may share such common fibril formation mechanisms, allowing inhibitors of one fibrillating protein to affect a completely different protein.

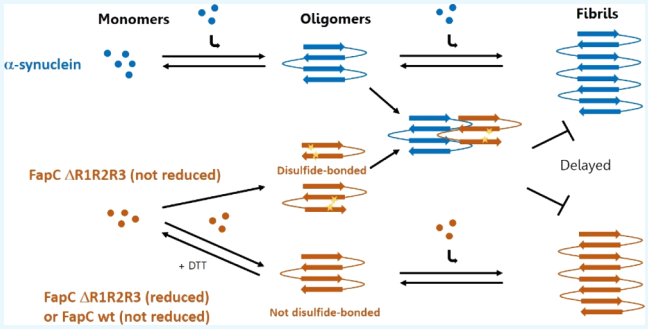

INTRODUCTION

Amyloid fibrils are nonbranched protein aggregates with a high content of β-sheets arranged so that the β-strands are perpendicular to the fibril axis.[1,2] They are often associated with neurodegenerative diseases such as Alzheimer's[3] and Parkinson's (PD),[4] where the brain accumulates intra- or extracellular deposits of misfolded protein. Fibril formation is a complex multistage mechanism with a sigmoidal time line, whose critical steps involve nucleation and elongation.[5,6] The rate-limiting step is the formation of oligomeric nuclei from monomeric precursors during the so-called lag phase. The nuclei can act as seeds and initiate fibril growth, leading to relatively fast fibril elongation once the nuclei have accumulated beyond a certain threshold level. This process continues until most of the soluble protein has been incorporated into the fibrils and there is an equilibrium between association and dissociation of monomeric protein at the fibril ends.

Amyloids also play useful roles in cell biology, particularly in bacteria where functional amyloid (FA) provides structural stability to bacterial biofilms,[7,8] forms protective sheaths,[9,10] or contributes to bacterial virulence.[11] These proteins are evolutionarily optimized to fibrillate and do not adopt a stable tertiary structure on the monomeric level but couple folding to fibrillation. Nevertheless, the time course of fibrillation remains sigmoidal[12,13] because of the need to accumulate and elongate the fibrillation nuclei.[14] The first FA to be described was CsgA, the main component of curli fibrils in *Escherichia coli* and other bacteria.[15,16] CsgA consists almost exclusively of five ∼20-residue imperfect repeats[17] connected by short four−five aa loop regions.[18] Each repeat is predicted to form a β-hairpin, all five of which stack on top of each other in the amyloid structure.[19] An unrelated FA system has been identified in *Pseudomonas* biofilms.[20] The main protein component in FAs in *Pseudomonas* (fap) is the FapC protein, which differs from CsgA in several ways. It contains only three ∼35-residue imperfect repeats (R1, R2, and R3), and these are connected by less well-conserved linker regions (L1 and L2) of variable (30−275 residues) lengths[20] and unknown functions. Stepwise removal of the three FapC repeats increases both fibrillation lag times and the tendency of the growing fibrils to fragment.[21] In CsgA, the repeats are also predicted to form a β-hairpin

Received: December 21, 2018
Accepted: February 11, 2019
Published: February 22, 2019

DOI: 10.1021/acsomega.8b03590
ACS Omega 2019, 4, 4029−4039

structure, which makes up the core of the mature fibrils,[22] whereas the linkers are proposed to form solvent-exposed flexible regions.[23] The increased length of FapC repeats leads to a fibril width of 4.5 nm as opposed to 3 nm for CsgA.[23] Unlike CsgA, FapC has a conserved C-terminal CXXC motif, which is not thought to be part of the fibril core but may promote interfiber connections.[23]

Both FapC and CsgA are expressed from dedicated FA operons that also encode chaperones, outer membrane proteins, and nucleator proteins.[16,20,22,24−26] The chaperone proteins help avoid intracellular aggregation[27] and ensure that the proteins are secreted as unstructured proteins.[28] Interestingly, two chaperone proteins from the curli system, CsgC and CsgH, share the same structural fold and inhibit fibrillation of not only CsgA but also FapC[29] and human α-synuclein (α-SN),[27,30] indicating similar features in the fibrillation of these proteins. The small-molecule epigallocatechin-3-gallate (EGCG) also inhibits fibrillation of both FapC,[31] human α-SN[32,33] and $A\beta_{42}$,[32] which is proposed to be involved in Alzheimer's disease. Interestingly, both the curli system chaperone CsgE and the small organic 2-pyridone compound named FN075 efficiently inhibit CsgA fibrillation,[34−36] but at the same time these molecules *accelerate* the fibrillation of human α-SN.[30,37] Altogether, these studies show that small molecules or proteins, probably due to common fibrillation mechanisms and the common cross-β structure of the mature amyloid fibrils, can affect different—and unrelated—amyloidogenic target proteins but that these interactions can result in opposite effects. Globular proteins are protected against amyloid fibrillation by their native fold, which sequesters amyloidogenic and hydrophobic regions of the proteins within the protein interior. Fibrillation requires conditions that favor protein unfolding or denaturation, leading to exposure of these regions and subsequent misfolding.[38] In contrast, intrinsically disordered proteins (IDPs) lack a stable tertiary structure[39] and therefore do not have the same barriers to aggregation. One such prominent IDP is the 140-residue protein α-SN, recognized for its involvement in PD, where it forms intracytoplasmic protein deposits referred to as Lewy bodies (LBs) or Lewy neurites (LNs). In the substantia nigra pars compacta of the midbrain, this results in a loss of dopaminergic neurons, ultimately leading to a number of motor symptoms.[40] In addition, gastrointestinal (GI) dysfunction is also commonly reported by PD patients,[41] indicating roles for the GI tract and the enteric nervous system (ENS) in PD. In fact, LBs and LNs are often observed in the neurons of the ENS in early stages of PD,[42−45] and recently the appendix was suggested to play an important role in PD initiation.[46]

Human α-SN has been shown to be transported retrogradely from the GI tract to the lower brain regions via the vagus nerve.[47,48] In the ENS, the great majority of neurons are located in the wall of the GI tract,[49] extend throughout the different layers of the GI tract, and connect directly with enteroendocrine cells,[50] which express various toll-like receptors and are able recognize different microbial structures.[51] As an example, curli fibrils are recognized by TLR1 and TLR2 and mediate interleukin 1β production,[52,53] and this way, the bacteria in our microbiome may interact with our central nervous system through the ENS. Rodent studies have shown that the bacterial composition in our microbiome or products produced by these bacteria can lead to increased α-SN deposition, possibly by activating the immune system or causing increased intestinal permeability, both within the GI tract[54,55] and in the brain.[56,57]

Feeding aged rats with curli-producing *E. coli* leads to an increase in α-SN aggregation compared to animals that had been fed with a curli-deficient *E. coli* strain,[57] indicating that microbiomic FAs contribute to PD pathogenesis. Because bacteria belonging to the genus *Pseudomonas* spp. have been found to be relatively abundant in healthy individuals,[58] we decided to search for evidence of any cross-interactions between FapC and human α-SN. To also study the role of imperfect repeats in wild-type FapC (henceforth referred to as FapC), we also included a FapC variant lacking all three repeats (FapC ΔR1R2R3). Although this mutant still forms thioflavin T (ThT)-positive amyloid-like fibrils, the process is significantly slower, and the resulting fibrils are thinner and more fragmented than their wild-type counterpart, not only confirming the importance of the repeats in driving fibrillation but also revealing a remarkable hidden amyloidogenicity in the linker regions. Remarkably, substoichiometric amounts of FapC ΔR1R2R3 delayed α-SN fibrillation up to 4-fold, whereas FapC had no effect. Because of the CXXC motif in both FapC and FapC ΔR1R2R3, the proteins could still form dimers, trimers, and higher order oligomers during purification; whereas suppression of disulfide bond formation under reducing conditions had no effect on FapC fibrillation, it significantly accelerated the fibrillation of FapC ΔR1R2R3 and at the same time abolished its ability to inhibit α-SN fibrillation. Thus, removal of the repeats slows down fibrillation to an extent where disulfide bond formation is favored. The disulfide-bonded protein species (dimers, trimers, and higher order oligomers) are able to interact with (and inhibit) both fibrillation of FapC ΔR1R2R3 itself and of human α-SN. The results presented here reveal how different fibrillation systems may share common fibril formation mechanisms, which allow for inhibitors of one system to affect a completely different system. In this specific case, the amyloidogenicity of FapC had to be reduced below a certain level to favor interaction with α-SN and inhibition of fibrillation. Thus, weakening the intrinsic, highly efficient aggregation mechanism of FA may exacerbate deleterious effects of otherwise benign amyloid.

MATERIALS AND METHODS

Purification of α-SN. Recombinant α-SN was expressed using autoinduction[59] and purified as previously described.[60]

α-SN Oligomer Formation. α-SN oligomers were purified as previously described.[61] Briefly, lyophilized α-SN was resuspended in a buffer to a final concentration of 8 mg/mL (∼0.55 mM) and incubated for 5 h at 37 °C while shaking with 900 rpm. After centrifugation (12 000*g*, 10 min, 4 °C), the sample was loaded on a Superose 6 10/300 GL column (GE Healthcare), and oligomer fractions were collected.

Design of the FapC Repeat Deletion Mutant Protein. FapC and FapC ΔR1R2R3 proteins were designed based on the FapC sequence from *Pseudomonas* strain UK4. The proteins were designed without the 24-residue N-terminal signal peptide and with a C-terminal 6xHis-tag. The amino acid sequences are included in Figure S1. Purification of His6-tagged FapC and FapC ΔR1R2R3: Recombinant FapC (vector: pET28a, kanamycin resistance) and FapC ΔR1R2R3 (vector: pET31b, ampicillin resistance) were purified as previously described[31] with a few modifications. In short, transformed *E. coli* BL21(DE3) cells (Bioneer A/S) were grown on LB agar plates for 24 h and then transferred to LB

DOI: 10.1021/acsomega.8b03590
ACS Omega 2019, 4, 4029−4039

medium containing antibiotics, 0.1% glucose, and 4 mM $MgSO_4$. Cells were grown to an OD_{600} of 0.6−0.8 before adding 1 mM isopropyl β-D-thiogalactopyranoside and allowing protein expression for 3 h. After cell harvest, the pellet was resuspended in 50 mL of denaturation buffer (8 M GdmCl, 50 mM Tris-HCl, pH 8.0) with one cOmplete protease inhibitor tablet (Roche) per L medium and lysed by slow stirring of the GdmCl-cell pellet suspension overnight at 4 °C. Cell debris was pelleted by ultracentrifugation (17 000*g*, 30 min, 15 °C), and the supernatant was incubated with freshly charged NiNTA beads for 1 h at 4 °C on a rolling table at 60 rpm. After washing the beads with first denaturation buffer and then with washing buffer (8 M GdmCl, 50 mM Tris-HCl, 30 mM imidazole, pH 8.0), the proteins were eluted into 2 mL fractions with elution buffer (8 M GdmCl, 50 mM Tris-HCl, 300 mM imidazole, pH 8.0). To check purity and protein content of the individual elutions, 5 μL of each elution was mixed with reducing loading buffer (G Biosciences) and 15 μL of Milli-Q (MQ) water and run on sodium dodecyl sulfate polyacrylamide gel electrophoresis (SDS-PAGE) gel. Eluted fractions were immediately frozen in liquid nitrogen and stored at −80 °C. Note that both FapC constructs contain a C-terminal His_6-extension to aid purification. The C-terminal part of FapC is not part of the imperfect repeat, which is thought to be part of the amyloid core, but is modelled in the recently computed structure of FapC to be highly mobile,[23] so we do not expect the attachment of an additional C-terminal His-tag to have any significant effect on fibrillation. In addition, we evaluate the impact of removal of the repeats within the same His-tagged background.

SDS-PAGE. Samples were boiled for 5 min at 95 °C, quickly spun down, and loaded on a 15% bistris SDS-polyacrylamide gel. The samples from the protein purification steps contained 2 M GdmCl, leading to precipitation in the loading buffer. We overcame this by pipetting up and down to homogenize the samples before loading them on the gel. Gels were run in a Bis-Tris running buffer at 150 V for 70 min, stained for 45 min in coomassie brilliant blue (CBB) (1.2 mM CBB, 5% ethanol, and 7% acetic acid), and destained overnight in a destaining solution (5% ethanol, 5% acetic acid).

ThT Fibrillation Assay. Monomers of purified FapC proteins were desalted from the elution buffer (8 M GdmCl, 50 mM Tris-HCl, 300 mM imidazole, pH 8.0) into phosphate-buffered saline (PBS) buffer in 0.5 mL fractions using a PD-10 desalting column (GE Healthcare). Lyophilized α-SN was dissolved in PBS buffer and filtered through a 0.2 μm filter. After measuring the concentration using a NanoDrop1000 (Thermo Scientific) spectrophotometer, the proteins were transferred to a black 96-well Nunc optical bottom plate (Thermo Scientific). Fibrillation followed with 40 μM ThT in a Tecan GENios Pro plate reader with excitation at 448 nm and emission at 485 nm. In case "clean" fibrils were needed (for dot blots), some wells were incubated without ThT. The program was run at 37 °C with 120 rpm and a measurement done every 124 s (FapC proteins alone) or with 600 rpm and a measurement done every 720 s (samples containing α-SN). Lag time was determined by normalizing the ThT fluorescence to 100%, by determining the slope of the linear part of the curve between 16 and 80% fluorescence and extrapolating its intersection with the *x*-axis. All samples were run in triplicate unless otherwise stated. For each FapC protein, the experiment was repeated three times. To estimate the extent of fibrillation after the end of incubation, the contents of different wells were thoroughly resuspended by pipetting and then centrifuged in a bench-top centrifuge at maximal speed (13.5 K rpm) for 15 min to pellet the insoluble material. The soluble fraction was run on SDS-PAGE and subjected to densitometric analysis with ImageJ. A control sample of monomeric FapC and FapC ΔR1R2R3 (prior to fibrillation) was included for normalization of data.

Fourier Transform Infrared Spectroscopy. The secondary structure of the protein aggregates/fibrils was analyzed with infrared spectroscopy using a Tensor 27 Fourier transform infrared (FTIR) instrument (Bruker Optics). The sample (2.0 μL) was deposited on an attenuated total reflection crystal, dried with nitrogen gas, and analyzed with the program OPUS version 5.5. Spectra were averaged over 68 scans in the 1000−3999 cm^{-1} range. Data were analyzed by calculating the atmospheric compensation, subtracting the baseline, and preparing the second-derivative spectra. Only the amide I band (1600−1700 cm^{-1}) is shown.

Transmission Electron Microscopy. The sample (5 μL) was applied to a 400-mesh carbon-coated glow-discharged Ni grid, and after 30 s, the grids were stained with 1% phosphotungstic acid (pH 7.0) and blotted dry on a filter paper. A transmission electron microscope (JEM-1010, JEOL) operating at 60 kV was used to view the samples, and images were obtained using an Olympus KeenViewG2 camera.

Dot Blots with Alexa Fluor 546 Reactive Dye. α-SN and FapC/FapCΔR1R2R3 fibrils were prepared by spinning down ThT-free fibrils and measuring the monomer concentration left in the supernatant. The fibril pellet was then resuspended to the desired concentration in the PBS buffer. To fragment the fibrils, they were sonicated briefly (α-SN fibrils) or for five cycles of 10 s with 10 s on ice in between (FapC/FapCΔR1R2R3 fibrils) using a Q125 sonicator with a 2 mm diameter probe (QSonica). Nitrocellulose membranes (0.2 μm, Bio-Rad) were either incubated with a dilution series of α-SN monomer, oligomer, and fibrils or with FapC/FapC ΔR1R2R3 monomers and fibrils. PBS buffer was included as a negative control. We used Ponceau S to verify that similar amounts of all of the bait proteins were bound to the membrane. Membranes were incubated with a Ponceau S solution (0.1% Ponceau S in 5% acetic acid) for 5 min with gentle agitation.[62] Subsequently, the membranes were washed with MQ water before blocking the membranes for 1 h with 0.5% bovine serum albumin (BSA) in PBS and washing them in washing buffer (0.05% Tween 20 in PBS buffer). After desalting into PBS buffer on a PD10 column, FapC or FapC ΔR1R2R3 monomers were incubated on ice (to minimize aggregation) for 1 h with Alexa Fluor 546 reactive dye (Thermo Fischer Scientific) according to the manufacturer's instructions. The leftover probe was removed in another desalting step, and 0.05 mg/mL (2.1 μM WT or 3.6 μM ΔR1R2R3) of labelled protein was incubated with the membrane for 2 h at room temperature. Finally, the membranes were washed in 0.05% Tween 20 and visualized using a Typhoon scanner 9410 (Amersham Biosciences) when dry. The procedure is summarized in Figure S2.

Size Exclusion Chromatography. To investigate the formation of mixed oligomers, 4 mg/mL (28 μM) α-SN with and without 2 mg/mL (84 or 144 μM) freshly desalted FapC/FapC ΔR1R2R3 was incubated with shaking (700 rpm) for 4.25 h at 37 °C in PBS and centrifuged (13 500*g*, 2 min) to remove larger aggregates. Then, 300 μL hereof was loaded on a Superose 6 10/300 GL column (GE Healthcare) with an

DOI: 10.1021/acsomega.8b03590
ACS Omega 2019, 4, 4029−4039

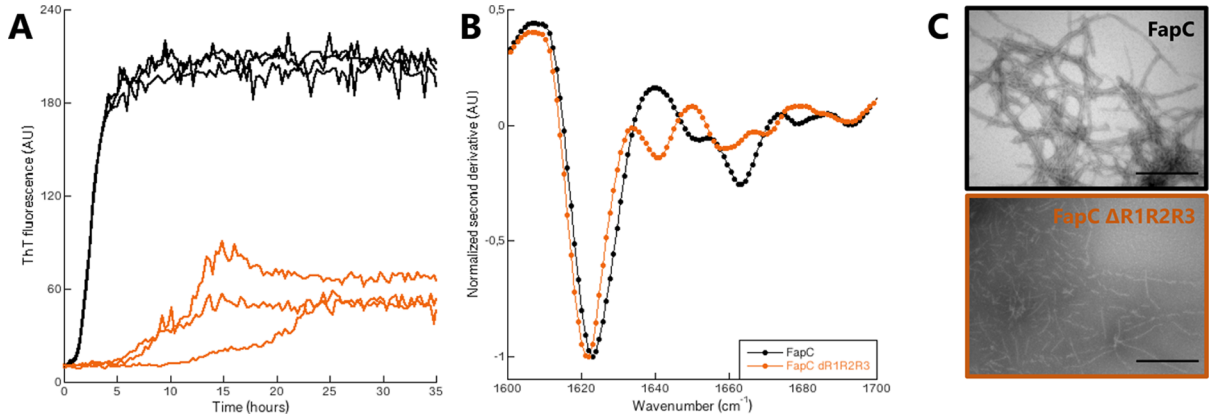

Figure 1. Both FapC and FapC ΔR1R2R3 form ThT-positive amyloid fibrils. (A) Fibrillation followed with ThT for 1 mg/mL FapC (=42 μM) (black) and 1 mg/mL FapC ΔR1R2R3 (=72 μM) (orange). After fibrillation, the fibrils were investigated with (B) FTIR and (C) TEM. The scale bar is 100 nm.

ÄKTA Pure protein purification system (GE Healthcare) at a flow rate of 0.5 mL/min. For samples containing FapC ΔR1R2R3, the experiments were repeated in the presence of 20 mM dithiothreitol (DTT), and 500 μL of fractions were collected.

Dot Blots with Antibodies. From the size exclusion chromatography (SEC) experiment, fractions 1−4 (elution volumes between 12.25 and 14.25 mL) (Figure 4A) containing the small oligomer were pooled and concentrated using a 0.5 mL Amicon centrifugation filter with a 30 K cutoff (Merck Millipore). Concentration was determined with a Pierce BCA protein assay kit (Thermo Scientific) following the manufacturer's instructions. The concentrated oligomers were then applied to two nitrocellulose membranes together with duplicates of 1 μg of freshly desalted FapC ΔR1R2R3 and 1 μg of monomeric human α-SN before the membranes were allowed to dry. PBS buffer was used as the control. After drying, the membranes were blocked with 0.5% BSA (w/v) in PBS buffer for 40 min at 4 °C before thoroughly washing them in the washing buffer. Primary antibodies were added to the membranes. One membrane was incubated with anti-α-SN mouse monoclonal IgG (Santa Cruz Biotechnology, catalog # sc-69977), and another membrane was incubated with anti-FapC rabbit polyclonal IgG.[63] Both the membranes were incubated for 1 h at room temperature. The membranes were washed in the washing buffer before adding the secondary antibodies against either mouse [horseradish peroxidase (HRP) goat anti-mouse IgG, #115-035-146] or rabbit (HRP goat anti-rabbit IgG, #111-035-144) (Jackson ImmunoResearch, USA) and incubated for an additional 1 h at room temperature. After washing the membranes in the washing buffer, protein binding was visualized using TMB Blotting PLUS solution (Kem-En-Tec Diagnostics A/S). Densitometric quantification was performed with ImageJ (https://imagej.net/).

Fibril Stability in Urea. FapC ΔR1R2R3 fibrils were made by incubating freshly desalted protein at 37 °C, 700 rpm for 48 h either with or without 20 mM DTT. Fibrils were spun down (13 500 rpm, 15 min) in a table centrifuge. The mass of pelleted protein fibrils was calculated based on the supernatant protein concentration (determined through A_{280}). The fibrils were resuspended in PBS to 1 mg/mL (72 μM in monomer units) and aliquoted into Eppendorf tubes. The fibrils were then pelleted again, and the supernatant was discarded before adding solutions of 8 M urea ±20 mM DTT. After 1 h at room temperature, the samples were again centrifuged, and 20 μL of each supernatant was transferred to a new Eppendorf tube and mixed with reducing loading buffer (G Biosciences). Samples were boiled for 5 min at 95 °C and run on SDS-PAGE together with a Mark12 unstained protein marker (Thermo Scientific) and control samples of 1 mg/mL (72 μM) freshly desalted FapC ΔR1R2R3 ± 20 mM DTT and 1 mg/mL (42 μM) wild-type FapC fibrils treated with 8 M urea ±20 mM DTT.

RESULTS

Both FapC and FapC ΔR1R2R3 Form ThT-Positive Amyloid Fibrils But with Differences in Morphology. We started by comparing the fibrillation properties of FapC and the repeat-less FapC mutant (FapC ΔR1R2R3) using the amyloid-binding dye ThT. Both proteins led to an increase in ThT fluorescence, but FapC ΔR1R2R3 showed a reduction in ThT fluorescence by a factor of 3.4 ± 0.5, a much longer lag phase and greater variation between individual runs (Figure 1A). The reduction in ThT fluorescence could be caused by a lower fibrillation yield, which in turn implies a larger population of soluble protein. To clarify this, we separated the solutions into soluble and insoluble components by centrifugation and estimated the amount of soluble protein by SDS-PAGE followed by densitometry. All soluble proteins migrated as monomers (data not shown). On the basis of triplicate measurements, 90 ± 5% of FapC fibrillated, but for FapC ΔR1R2R3, this was reduced to 44 ± 4%, that is, a 2-fold reduction in yield, which nevertheless is smaller than the 3.4-fold reduction in ThT fluorescence. Thus, the reduction in ThT fluorescence must be ascribed to both reduction in yield as well as change in the fibril structure, which affects ThT fluorescence. Nevertheless, both variants gave rise to FTIR spectra with a pronounced peak around 1620 cm^{-1} (Figure 1B). This is taken to indicate an amyloid cross-β structure; the greater size and higher order of the β-sheets in the amyloid fibrils shift the frequencies to lower wavenumbers compared to conventional β-sheets which absorb >1630 cm^{-1}.[64] The presence of fibrillar structures for both proteins was also confirmed with transmission electron microscopy (TEM) (Figure 1C). Fibrils formed from FapC ΔR1R2R3 were generally smaller, thinner, and more fragmented than the FapC

DOI: 10.1021/acsomega.8b03590
ACS Omega 2019, 4, 4029−4039

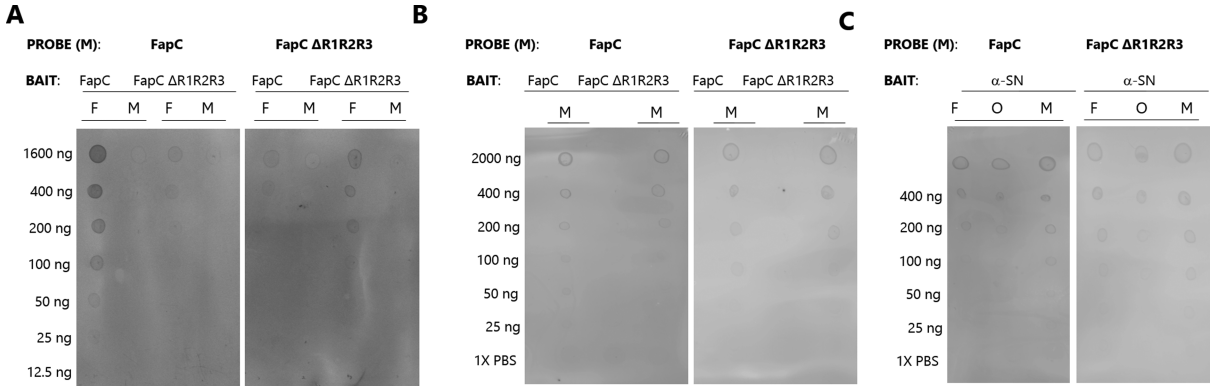

Figure 2. Monomers of FapC and FapC ΔR1R2R3 both preferentially recognize their own fibrils and recognize different species of α-SN. Dot blot of labelled FapC (left) or labelled FapC ΔR1R2R3 (right) binding to 12.5−2000 ng of (A) immobilized monomers (M) or fibrils (F) of either FapC or FapC ΔR1R2R3 and decreasing concentrations of (B) immobilized FapC/FapC ΔR1R2R3 monomers or (C) immobilized α-SN monomers, oligomers (O), and fibrils.

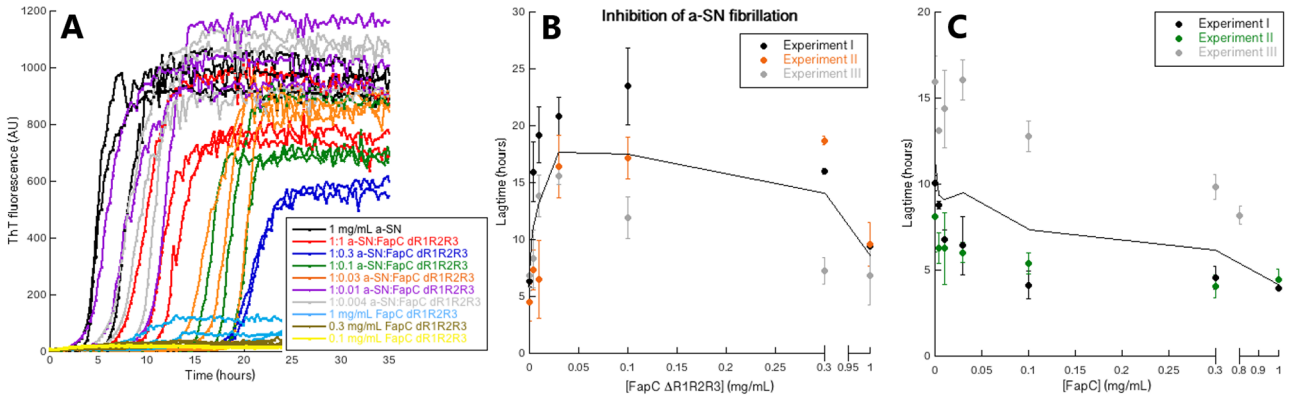

Figure 3. Inhibition of α-SN fibrillation by FapC ΔR1R2R3. (A) Fibrillation of 1 mg/mL α-SN (69 μM) in the presence of monomeric FapC ΔR1R2R3 at concentrations ranging from 0.004 mg/mL (0.3 μM) to 1 mg/mL (72 μM). Lag time of α-SN fibrillation as a function of (B) FapC ΔR1R2R3 or (C) FapC concentration. Data using monomeric FapC or FapC ΔR1R2R3 are from three individual experiments I−III (each in triplicate). The average from these three experiments is shown with a black line. Results from experiments using fibrils of FapC or FapC ΔR1R2R3 instead of monomeric protein are shown in green and indicate no significant effect.

fibrils, and this altered morphology may explain the reduction in ThT fluorescence in Figure 1A.

Monomeric FapC Has High Affinity for Its Own Fibrils. To investigate interactions between monomeric and fibrillary FapC, we incubated Alexa 546-labelled FapC/FapC ΔR1R2R3 monomer as a probe with membranes, on which we had immobilized both FapC and FapC ΔR1R2R3 as bait in monomeric (M) and in fibrillar (F) forms. To control the extent of bait binding, we stained the membranes with Ponceau S prior to the analysis. Fibrils bound to a 2−4-fold smaller extent than monomers, but both variants bound to essentially the same extent (Figure S3). FapC monomers bind preferentially to FapC fibrils, leaving very little to bind to the FapC ΔR1R2R3 fibrils (Figure 2A, left). Monomeric FapC ΔR1R2R3 also preferably binds its own fibrils but shows less overall binding than FapC (Figure 2A, right), nicely consistent with FapC ΔR1R2R3's lower aggregation tendency (Figure 1A). We ascribe the lack of binding to immobilized monomeric proteins to the much higher affinity of the monomer toward the fibrils that are present in the same binding reaction. In the absence of immobilized fibrils, both labelled FapC/FapC ΔR1R2R3 monomers bind both types of monomers (Figure 2B).

Both FapC and FapC ΔR1R2R3 Bind to All Species of Human α-SN But Only FapC ΔR1R2R3 Inhibits α-SN Fibrillation. Because of the possible link between the human microbiome and PD spreading and pathology, we speculated whether wild-type FapC and FapC ΔR1R2R3 monomers recognize and interact with human α-SN. CsgC/CsgH and EGCG inhibit fibrillation of both FapC and human α-SN, indicating that FapC and α-SN share common structural features.[27,29−32] We were unable to investigate interactions between the different proteins by conventional biophysical approaches such as Biacore or Isothermal Titration Calorimetry because of the relatively large quantities of homogeneous sample needed as well as the rather weak binding interactions. However, as a first step to investigate these possible interactions, we immobilized both monomeric, oligomeric, and fibrillar α-SN on membranes and exposed them to labelled, monomeric FapC/FapC ΔR1R2R3. Remarkably, both FapC proteins could recognize all types of α-SN, with no clear preference for one particular species (Figure 2C). This opened up the possibility that they might also affect α-SN fibrillation. We therefore incubated a constant amount (1 mg/mL or 70 μM) of α-SN with 0−1 mg/mL (0−72 μM) FapC ΔR1R2R3. As shown in Figure 3A,B, α-SN/FapC ΔR1R2R3 ratios between 1:0.03 and 1:0.3 (in ratios of mg/mL, essentially identical to molar ratios) increased the lag time of α-SN fibrillation by 2−4-fold. The effect diminished at higher FapC ΔR1R2R3 concentrations, which we interpret as a

DOI: 10.1021/acsomega.8b03590
ACS Omega 2019, 4, 4029−4039

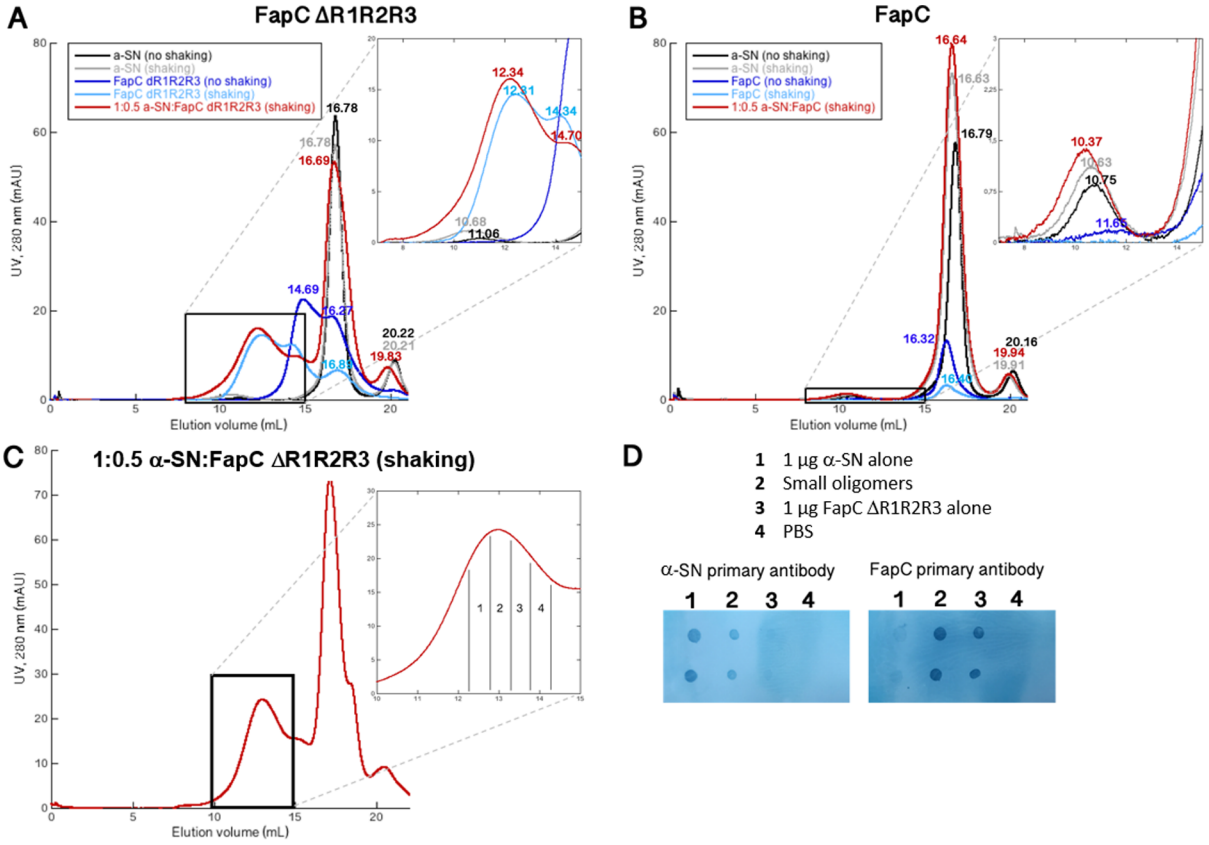

Figure 4. FapC ΔR1R2R3 forms small, mixed oligomers with α-SN. α-SN (4 mg/mL, 275 μM) and either (A) 2 mg/mL FapC ΔR1R2R3 (145 μM) or (B) 2 mg/mL FapC (85 μM) were run on SEC before (no shaking) and after shaking (4.25 h, 37 °C, 700 rpm). α-SN was run either alone or in a α-SN/FapC ΔR1R2R3 ratio of 1:0.5. Notice the difference in the $UV_{280\ nm}$ of the zoomed graphs. Numbers represent the precise elution volumes (in mL) obtained from the Gaussian fitting to the elution profiles. (C) From the SEC run with 1:0.5 α-SN/FapC ΔR1R2R3 after shaking, fractions 1−4 (zoom) were collected. (D) All four fractions were pooled, up-concentrated and immobilized on nitrocellulose membranes together with duplicates of 1 μg α-SN, 1 μg freshly desalted FapC ΔR1R2R3, and 1× PBS and investigated with antibodies against either α-SN (left) or FapC (right).

preference for FapC−FapC interactions as opposed to FapC-α-SN interactions. A substoichiometric optimum for inhibition is also consistent with the ability of monomeric FapC to interact with aggregated species of α-SN (Figure 2C). In contrast, FapC was not able to inhibit α-SN fibrillation; rather, it slightly accelerated α-SN fibrillation in a concentration-dependent manner (Figures 3C and S4). Two other mutants of FapC, namely FapC ΔR3 and FapC ΔR1R3 lacking one and two repeats, respectively, fibrillated at rates very comparable to FapC and were also unable to inhibit α-SN fibrillation (data not shown). This indicates that FapC needs to be significantly impaired in its fibrillation to inhibit α-SN fibrillation. In addition to monomeric FapC, we also tested the effect of adding different amounts (0−0.35 mg/mL, i.e., 0−15/25 μM in monomeric units) of fibrillated FapC and FapC ΔR1R2R3 to 1 mg/mL (70 μM) monomeric α-SN but found no significant effect on aggregation (Figure 3), indicating that FapC ΔR1R2R3 needs to be able to access the monomeric state to inhibit α-SN aggregation.

Small Oligomers Are Formed When Incubating α-SN with FapC ΔR1R2R3. We reasoned that FapC ΔR1R2R3 could delay α-SN fibrillation by trapping α-SN in a hetero-oligomeric state. Therefore, we incubated 1:0.5 (mass/mass) α-SN and FapC ΔR1R2R3 at 37 °C with agitation for ∼4 h before running the samples on a size exclusion column to analyze the size distribution of the ensuing aggregates. Coincubation leads to two peaks at 12.23 and 14.40 mL (monomeric α-SN elutes at 17 mL) (Figure 4A, red curve), and we will refer to the 12.23 mL peak as the small oligomer peak. These two peaks are only slightly changed compared to the two peaks formed around 12.42 and 14.15 mL by FapC ΔR1R2R3 alone after 4 h of shaking (Figure 4A, light blue curve). Inspecting the elution profile of the coincubation (red curve in Figure 4A), the α-SN monomer peak at 16.69 mL has not increased in intensity compared to that of FapC-free α-SN (gray curve), although monomeric FapC ΔR1R2R3 elutes at 16.89 mL. It should, however, be noticed that the red 16.69 mL peak has broadened compared to FapC-free α-SN, making it fair to assume that protein is eluting both as monomeric α-SN and monomeric FapC ΔR1R2R3. Even right after desalting, FapC ΔR1R2R3 does not exist exclusively as a monomer (Figure 4A, dark blue curve); in addition to the monomer peak around 16.55 mL (close to the value of monomeric α-SN, in good agreement with 124 and 140 residues for FapC ΔR1R2R3 and α-SN, respectively), there is a large peak around 14.86 mL. We speculated that this oligomerization could be due to disulfide bond formation between cysteine residues in the C-terminal $C_{112}XXC_{115}$ motif of FapC ΔR1R2R3 (Figure S1). This was confirmed by incubating FapC ΔR1R2R3 with the reducing agent DTT, leading to loss of the 12 mL peak and a strong reduction in the size of the 14 mL peak, that is, the protein now eluted

DOI: 10.1021/acsomega.8b03590
ACS Omega 2019, 4, 4029−4039

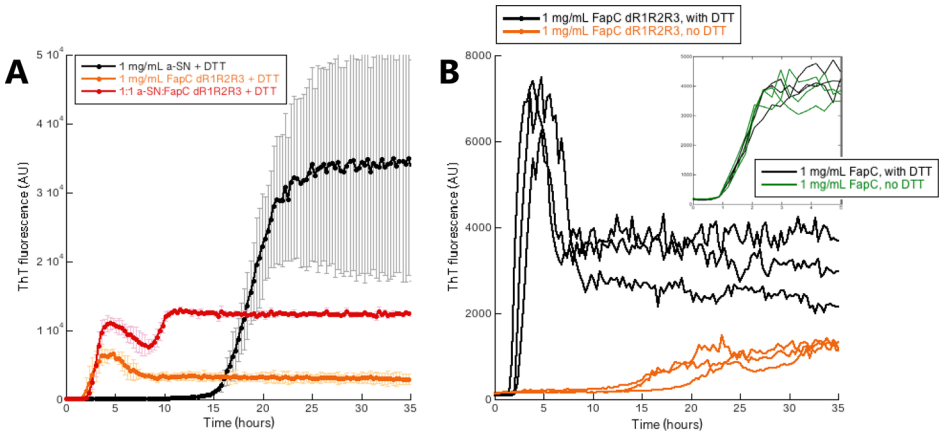

Figure 5. Inhibitory effect of FapC ΔR1R2R3 on α-SN fibrillation is lost under reducing conditions. (A) Fibrillation of 1 mg/mL α-SN (69 μM) in the presence of FapC ΔR1R2R3 concentrations ranging from 0.004 mg/mL (0.3 μM) to 1 mg/mL (72 μM) in the presence of DTT. (B) Effect of DTT on the fibrillation kinetics of FapC ΔR1R2R3 and (inset) FapC.

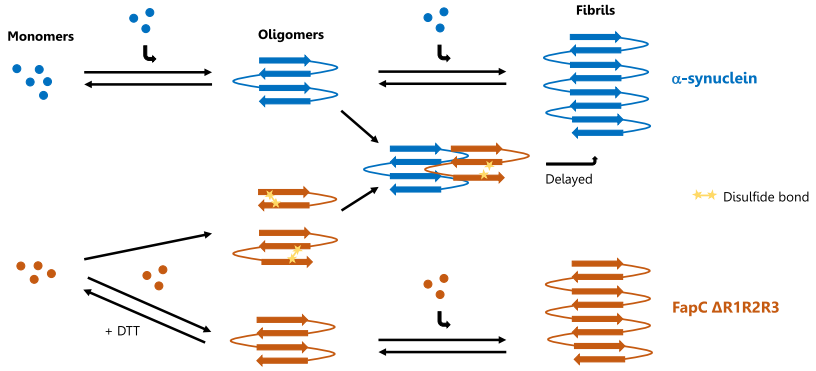

Figure 6. Proposed mechanism for inhibition of α-SN fibrillation by FapC ΔR1R2R3. For both α-SN (blue) and FapC ΔR1R2R3 (orange), monomers (spheres) can form oligomers that can be elongated further to mature fibrils. Because of its long lag phase, FapC ΔR1R2R3 will start forming dimers, trimers, and oligomers with disulfide bond linkages (yellow stars), and these species retard fibrillation of FapC ΔR1R2R3 itself as well as α-SN.

exclusively as a monomer at 17.34 mL with approximately the same molecular weight as α-SN (Figure S5A, blue curve). When α-SN and FapC ΔR1R2R3 were coincubated, DTT also inhibited the formation of small oligomers and instead gave rise to an elution profile that was a combination of monomeric α-SN and reduced, monomeric FapC ΔR1R2R3 (Figure S5B, light green curve). Incubation of α-SN with FapC did not have any significant effect on oligomer formation (Figure 4B, red curve) beyond a very small increase in the peak height and a small shift to earlier elution volumes (from 10.67 to 10.51 mL).

Small Oligomers Are Composed Primarily of FapC ΔR1R2R3 But Also Contain α-SN. To confirm the content of FapC ΔR1R2R3 in the small oligomers, we concentrated the oligomer fractions 1−4 between elution volumes 12.25 and 14.25 mL (Figure 4C) and immobilized them on nitrocellulose membranes. Two identical membranes were produced and probed with antibodies against either human α-SN or FapC. Monomeric α-SN, freshly desalted FapC ΔR1R2R3, and PBS were included as controls. These blots clearly showed that the small oligomers contained high amounts of FapC ΔR1R2R3 but that α-SN was also present as a minor component (Figure 4D), again indicating direct interaction between FapC ΔR1R2R3 and α-SN. On the basis of the densitometric analysis, we estimated the amount of FapC ΔR1R2R3 and α-SN in the spot (fractions 1−4) to be 1.38 ± 0.02 and 0.41 ± 0.06 μg, respectively, giving a FapC ΔR1R2R3/α-SN mass ratio of 3.4:1 (Figure 4D). α-SN oligomers elute around 10.67 mL, indicating that we have formed α-SN/FapC ΔR1R2R3 hetero-oligomers (Figure 4B). That some α-SN is eluting already between 12.25 and 14.25 mL as part of these small oligomers is also consistent with the small decline in the α-SN peak in the α-SN/FapC ΔR1R2R3 coincubation SEC elution profile (Figure 4A, red and gray curves).

Ability of FapC ΔR1R2R3 To Inhibit α-SN Fibrillation Depends on Disulfide Bond Formation. Finally, we investigated if disulfide bond formation by FapC ΔR1R2R3 was essential for its ability to inhibit human α-SN fibrillation. α-SN was again incubated with different ratios of FapC ΔR1R2R3, and DTT was included to inhibit disulfide bond formation. Reducing conditions completely abolished the inhibitory effect (Figure 5A). In this figure, the red curve portraying the fibrillation of the α-SN/FapC ΔR1R2R3 mixture contains both a rapid rise and a slow descent (ca. 2−7 h) corresponding to the behavior of free FapC ΔR1R2R3 (orange curve) and a subsequent fibrillation (reaching a plateau around 10 h), which corresponds to free α-SN. α-SN thus fibrillates even more rapidly in the presence of reduced FapC ΔR1R2R3 than alone, that is, it is not inhibited. Remarkably, the reduction of FapC ΔR1R2R3 also completely changed its fibrillation pattern, and now the protein fibrillated extremely fast as opposed to its normal fibrillation behavior

DOI: 10.1021/acsomega.8b03590
ACS Omega 2019, 4, 4029−4039

(Figure 5B). This suggests that the lack of imperfect repeats, leading to a longer fibrillation lag phase, allows for disulfide bond formation and that these bonds halt FapC ΔR1R2R3 in various dimers, trimers, or higher order oligomers and thereby complicate fibrillation. The change in fibrillation kinetics, however, affected neither the structure nor the stability of the mature fibrils: FapC ΔR1R2R3 fibrils formed with or without DTT give similar FTIR spectra (Fig S6A) and dissolve to the same extent in 8 M urea ± DTT (Figure S6B, compare lanes 6−7 and lanes 10−11). Figure 6B demonstrates that removing all repeats from FapC significantly affects the stability of the mature fibrils: wild-type FapC fibrils are completely resistant toward 8 M urea ± DTT (lanes 14 + 15) and require more harsh solvents such as formic acid to dissolve.[20,65] Incubating FapC with DTT did not affect fibrillation (Figure 5B, inset). Consistent with this, mutating away the CXXC motif in FapC from *Pseudomonas aeruginosa* PAO1 does not affect fibrillation.[12]

DISCUSSION

Imperfect repeats in the sequences of FA proteins such as CsgA and FapC are believed to be the main drivers of amyloid formation. To investigate the importance of these repeats, we designed a mutant of FapC where all three imperfect repeats were removed (FapC ΔR1R2R3) and showed that this mutant protein was still able to form ThT-positive fibrillar structures that showed amyloid-characteristic secondary structure when investigated with FTIR. However, the fibrillation lag phase was considerably longer for FapC ΔR1R2R3, the yield and ThT-binding properties of this mutant's fibrils were reduced several fold compared to wild-type, and the fibrils were thinner, shorter, and more fragmented when compared to fibrils formed by FapC. This indicated a marked reduction in both quantity and quality of fibrillation by the removal of these repeats. Both FapC and FapC ΔR1R2R3 have a C-terminal CXXC motif (which is conserved among pseudomonads) (Figure S1), and it was recently shown that these residues are not required for polymerization of FapC from *P. aeruginosa* PAO1, as replacement of the Cys residues with Ser or Glu residues did not affect either the fibrillation rate, extent, or fibril structure.[12] The same has been observed for a Cys-less mutant of FapC from the *Pseudomonas* strain UK4 (B.S.V., unpublished results). In contrast, FapC ΔR1R2R3 fibrillation in the presence of the reducing agent DTT was markedly accelerated, leading to a lag phase reduction from ∼12 to <2 h, much more resembling the lag phase seen for FapC. This indicates that disulfide bonds formed between FapC ΔR1R2R3 molecules, favored by the extended lag phase, trap FapC ΔR1R2R3 proteins in off-pathway structures, which in turn inhibits fibrillation and leads to formation of less well-structured aggregates with lower ThT fluorescence and thinner fibrils.

It has been suggested that the GI tract could be a possible initiation site for PD pathogenesis because of the early appearance of α-SN aggregates in GI tissues.[44−46] One possibility is that this is a response to the bacteria in our microbiome,[56,66] many of which form FA that are structurally similar to α-SN fibrils.[67] To study possible interactions between the FA protein FapC and α-SN, we incubated α-SN with both FapC and the FapC ΔR1R2R3 mutant. Incubating human α-SN with FapC ΔR1R2R3 revealed that certain ratios of α-SN/FapC ΔR1R2R3 led to an almost 4-fold increase in the α-SN fibrillation lag phase, whereas FapC had no effect on α-SN fibrillation. This inhibiting effect of FapC ΔR1R2R3 was dependent on disulfide bond formation as the effect was lost when we repeated the experiment with DTT present. We therefore propose a mechanism wherein FapC ΔR1R2R3 molecules, because of its long lag phase, can form dimers, trimers, and oligomers with disulfide bond linkages. These disulfide-bonded species are then able to interact with α-SN (probably in its oligomeric form because the inhibition is optimal at substoichiometric ratios of α-SN/FapC ΔR1R2R3), thereby inhibiting α-SN fibrillation (Figure 6). That α-SN fibril formation was not entirely prevented, but just delayed, indicates that the α-SN monomers are not irreversibly trapped by the disulfide-bonded FapC ΔR1R2R3 oligomeric species but can rearrange to eventually form fibrils. This could indicate some kind of transient contacts between FapC ΔR1R2R3 and α-SN, similar to what has been suggested in the inhibition of α-SN by CsgC.[30] When α-SN was incubated with FapC ΔR1R2R3 and run on a size exclusion column, we were able to isolate small oligomers containing primarily FapC ΔR1R2R3 as well as α-SN. This indicates that the two proteins interact directly because it appears that FapC ΔR1R2R3 to some degree is able to complex α-SN, which otherwise does not elute between 12.25 and 14.25 mL (Figure 4A,B). No increase in oligomer formation was observed when human α-SN was incubated together with FapC. We speculate that this is because the fast fibrillation kinetics for FapC allows it to fibrillate independently of α-SN. To summarize, the amyloidogenicity of FapC had to be reduced below a certain level (which was only seen for the most amputated of the FapC mutants: FapC ΔR1R2R3) to favor the interaction with and inhibition of α-SN fibrillation. It is unlikely that this will have any direct relevance for our understanding of the biological role of FapC. Even though *Pseudomonas* is found in the gut, wild-type FapC aggregates very rapidly and does not react directly with α-SN, according to our experiments, so the FapC secreted from the bacterium will likely be integrated into the growing fibrils well before it even encounters any free α-SN. However, our data emphasize that cross-talk can depend on the rapidity of the fibrillation process, so that retardation of fibrillation or intermediate aggregate structures trapped under in vivo conditions could in fact promote interactions with other fibrillating species.

The results presented here provides a new twist on the role of 31- and 30-residue long linkers in FapC from *Pseudomonas* strain UK4. In the current model of the mature Fap fibrils, the imperfect repeats form the core of the fibrils while the linker regions are exposed to the surrounding environment.[22,23] However, since FapC ΔR1R2R3 is still capable of forming fibril structures, some fibrillation information must be encoded within these linkers. It remains to be investigated whether this is unique to UK4 FapC or if it is also true for FapC homologs from other pseudomonads. Comparison of the linker sequences of different FapC proteins shows that especially L2 is highly variable in size[20] but that both L1 and L2 contain conserved asparagine, glutamine, and alanine residues (Figure S7). Conservation of these amino acids are also observed in the FapC repeat regions[20] and in other amyloidogenic proteins such as CsgA,[17,68] prion,[69] and spider silk proteins[70] and could partly explain the amyloidogenicity of the linkers. A simple explanation for the residual fibrillation propensity of FapC ΔR1R2R3 is that the repeat sequences drive amyloid formation so strongly that the linkers' intrinsic fibrillation propensity lies dormant and can only be manifested in the absence of these repeats.

DOI: 10.1021/acsomega.8b03590
ACS Omega 2019, 4, 4029−4039

Not only does the results presented here shed light on the FapC fibrillation mechanism but they also emphasize how one fibrillating protein may affect a completely different protein because the systems share common fibril formation mechanisms. A different example of such cross-interactions is the ability of the human amyloid precursor transthyretin to inhibit unrelated proteins such as Aβ_{40}[71] and CsgA,[72] suggesting that the primary sequences and the species of origin of the proteins are less important than the fibrillation mechanism itself. Coincubation of different fibrillation proteins can also result in *increased* fibril formation as in the case of tau and the α-SN mutant A53T (α-SN$_{A53T}$) protein. Both proteins fibrillate independently (even though tau requires the presence of cofactors such as sulphated glycosaminoglycans[73,74]), but coincubation of the two proteins results in increased formation of both α-SN and tau inclusions.[74] As both tau and α-SN are involved in neurodegenerative diseases, studies such as this one open up the possibility that therapeutic agents that effectively inhibit one form of amyloid might also be effective in the treatment of other neurological disorders.

■ ASSOCIATED CONTENT

Supporting Information

The Supporting Information is available free of charge on the ACS Publications website at DOI: 10.1021/acsomega.8b03590.

FapC and FapC ΔR1R2R3 protein sequences, dot-blot setup, cross-recognition between FapC and FapC ΔR1R2R3, ThT time profiles showing lack of inhibition of α-SN fibrillation by FapC, formation of FapC ΔR1R2R3 disulfide-bonded oligomers according to gel filtration, stability of FapC ΔR1R2R3 fibrils in urea, and sequence analysis of repeats and linker regions in FapC (PDF)

■ AUTHOR INFORMATION

Corresponding Author

*E-mail: dao@inano.au.dk.

ORCID

Daniel Erik Otzen: 0000-0002-2918-8989

Notes

The authors declare no competing financial interest.

■ ACKNOWLEDGMENTS

D.O. and L.F.B.C. are funded by Innovation Foundation Denmark (Grant 5188-00003B) through the Joint Programme on Neurodegenerative Diseases (aSynProtec) coordinated by Prof. Jia-Yi Li.

■ ABBREVIATIONS

α-SN, α-synuclein; BSA, bovine serum albumin; CNS, central nervous system; DTT, dithiothreitol; EGCG, epigallochatechin-3-gallate; ENS, enteric nervous system; FapC, major functional amyloid protein in *Pseudomonas*; FTIR, Fourier-transform infrared; GdmCl, guanidine hydrochloride; GI, gastrointestinal; HRP, horseradish peroxidase; IDPs, intrinsically disordered proteins; LBs, Lewy bodies; LNs, Lewy neurites; MAMPs, microbe-associated molecular patterns; MQ, Milli-Q; PD, Parkinson's disease; SEC, size-exclusion chromatography; TTR, transthyretin

■ REFERENCES

(1) Sipe, J. D.; Benson, M. D.; Buxbaum, J. N.; Ikeda, S.-i.; Merlini, G.; Saraiva, M. J. M.; Westermark, P. Nomenclature 2014: Amyloid fibril proteins and clinical classification of the amyloidosis. *Amyloid* **2014**, *21*, 221−224.

(2) Chiti, F.; Dobson, C. M. Protein Misfolding, Amyloid Formation, and Human Disease: A Summary of Progress Over the Last Decade. *Annu. Rev. Biochem.* **2017**, *86*, 27−68.

(3) Finder, V. H.; Glockshuber, R. Amyloid-β Aggregation. *Neurodegener. Dis.* **2007**, *4*, 13−27.

(4) Fink, A. L. The Aggregation and Fibrillation of α-Synuclein. *Acc. Chem. Res.* **2006**, *39*, 628−634.

(5) Lee, C.-C.; Nayak, A.; Sethuraman, A.; Belfort, G.; McRae, G. J. A three-stage kinetic model of amyloid fibrillation. *Biophys. J.* **2007**, *92*, 3448−3458.

(6) Cohen, S. I.; Vendruscolo, M.; Dobson, C. M.; Knowles, T. J. The Kinetics and Mechanisms of Amyloid Formation. In *Amyloid Fibrils and Prefibrillar Aggregates: Molecular and Biological Properties*; Otzen, D. E., Ed.; Wiley-VCH Verlag GmbH & Co. KGaA, 2013.

(7) Romero, D.; Aguilar, C.; Losick, R.; Kolter, R. Amyloid fibers provide structural integrity to Bacillus subtilis biofilms. *Proc. Natl. Acad. Sci. U.S.A.* **2010**, *107*, 2230.

(8) Fowler, D. M.; Koulov, A. V.; Kelly, J. W. Functional amyloid - from bacteria to humans. *Trends Biochem. Sci.* **2007**, *32*, 217−224.

(9) Dueholm, M. S.; Larsen, P.; Finster, K.; Stenvang, M. R.; Christiansen, G.; Vad, B. S.; Bøggild, A.; Otzen, D. E.; Nielsen, P. H. The Tubular Sheaths EncasingMethanosaeta thermophilaFilaments Are Functional Amyloids. *J. Biol. Chem.* **2015**, *290*, 20590−20600.

(10) Christensen, L. F. B.; Hansen, L. M.; Finster, K.; Christiansen, G.; Nielsen, P. H.; Otzen, D. E.; Dueholm, M. The Sheaths of Methanospirillum Are Made of a New Type of Amyloid Protein. *Front. Microbiol.* **2018**, *9*, 2729.

(11) Van Gerven, N.; Van der Verren, S. E.; Reiter, D. M.; Remaut, H. The Role of Functional Amyloids in Bacterial Virulence. *J. Mol. Biol.* **2018**, *430*, 3657−3684.

(12) Bleem, A.; Christiansen, G.; Madsen, D. J.; Maric, H.; Strømgaard, K.; Bryers, J. D.; Daggett, V.; Meyer, R. L.; Otzen, D. E. Protein Engineering Reveals Mechanisms of Functional Amyloid Formation in Pseudomonas aeruginosa Biofilms. *J. Mol. Biol.* **2018**, *430*, 3751−3763.

(13) Dueholm, M. S.; Nielsen, S. B.; Hein, K. L.; Nissen, P.; Chapman, M.; Christiansen, G.; Nielsen, P. H.; Otzen, D. E. Fibrillation of the major curli subunit CsgA under a wide range of conditions implies a robust design of aggregation. *Biochemistry* **2011**, *50*, 8281−8290.

(14) Andreasen, M.; Meisl, G.; Taylor, J. D.; Michaels, T. C. T.; Otzen, D. E.; Chapman, M.; Dobson, C. M.; Matthews, S.; Knowles, T. P. J. Physical determinants of amyloid assembly in biofilm formation. *mBio* **2019**, *10*, No. e02279.

(15) Collinson, S. K.; Emödy, L.; Müller, K. H.; Trust, T. J.; Kay, W. W. Purification and characterization of thin, aggregative fimbriae from Salmonella enteritidis. *J. Bacteriol.* **1991**, *173*, 4773−4781.

(16) Chapman, M. R.; Robinson, L. S.; Pinkner, J. S.; Roth, R.; Heuser, J.; Hammar, M.; Normark, S.; Hultgren, S. J. Role of Escherichia coli curli operons in directing amyloid fiber formation. *Science* **2002**, *295*, 851−855.

(17) Wang, X.; Chapman, M. R. Sequence determinants of bacterial amyloid formation. *J. Mol. Biol.* **2008**, *380*, 570−580.

(18) Hammer, N. D.; Schmidt, J. C.; Chapman, M. R. The curli nucleator protein, CsgB, contains an amyloidogenic domain that directs CsgA polymerization. *Proc. Natl. Acad. Sci. U.S.A.* **2007**, *104*, 12494−12499.

(19) Tian, P.; Boomsma, W.; Wang, Y.; Otzen, D. E.; Jensen, M. H.; Lindorff-Larsen, K. Structure of a Functional Amyloid Protein Subunit Computed Using Sequence Variation. *J. Am. Chem. Soc.* **2014**, *137*, 22−25.

(20) Dueholm, M. S.; Petersen, S. V.; Sonderkaer, M.; Larsen, P.; Christiansen, G.; Hein, K. L.; Enghild, J. J.; Nielsen, J. L.; Nielsen, K.

DOI: 10.1021/acsomega.8b03590
ACS Omega 2019, 4, 4029−4039

L.; Nielsen, P. H.; Otzen, D. E. Functional amyloid in Pseudomonas. *Mol Microbiol* **2010**, *77*, 1009−20.
(21) Rasmussen, C.; Christiansen, G.; Vad, B. S.; Enghild, J. J.; Lynggaard, C.; Andreasen, M.; Otzen, D. E. Imperfect repeats in the functional amyloid protein FapC reduce the tendency to secondary nucleation and fragmentation during fibrillation. *Protein Sci.* **2019**, *28*, 633.
(22) Dueholm, M. S.; Søndergaard, M. T.; Nilsson, M.; Christiansen, G.; Stensballe, A.; Overgaard, M. T.; Givskov, M.; Tolker-Nielsen, T.; Otzen, D. E.; Nielsen, P. H. Expression of Fap amyloids inPseudomonas aeruginosa,P. fluorescens,andP. putidaresults in aggregation and increased biofilm formation. *MicrobiologyOpen* **2013**, *2*, 365−382.
(23) Rouse, S. L.; Matthews, S. J.; Dueholm, M. S., Ecology and Biogenesis of Functional Amyloids in Pseudomonas. *J. Mol. Biol.* **2018**, *430*, 3685. DOI: 10.1016/j.jmb.2018.05.004
(24) Hammar, M. r.; Arnqvist, A.; Bian, Z.; Olsén, A.; Normark, S. Expression of two csg operons is required for production of fibronectin- and congo red-binding curli polymers in Escherichia coli K-12. *Mol. Microbiol.* **2004**, *18*, 661−670.
(25) Taylor, J. D.; Zhou, Y.; Salgado, P. S.; Patwardhan, A.; McGuffie, M.; Pape, T.; Grabe, G.; Ashman, E.; Constable, S. C.; Simpson, P. J.; Lee, W.-c.; Cota, E.; Chapman, M. R.; Matthews, S. J. Atomic resolution insights into curli fiber biogenesis. *Structure* **2011**, *19*, 1307−1316.
(26) Dueholm, M. S.; Otzen, D.; Nielsen, P. H. Evolutionary insight into the functional amyloids of the pseudomonads. *PLoS One* **2013**, *8*, No. e76630.
(27) Evans, M. L.; Chorell, E.; Taylor, J. D.; Åden, J.; Götheson, A.; Li, F.; Koch, M.; Sefer, L.; Matthews, S. J.; Wittung-Stafshede, P.; Almqvist, F.; Chapman, M. R. The bacterial curli system possesses a potent and selective inhibitor of amyloid formation. *Mol. Cell* **2015**, *57*, 445−455.
(28) Barnhart, M. M.; Chapman, M. R. Curli biogenesis and function. *Annu. Rev. Microbiol.* **2006**, *60*, 131−147.
(29) Taylor, J. D.; Hawthorne, W. J.; Lo, J.; Dear, A.; Jain, N.; Meisl, G.; Andreasen, M.; Fletcher, C.; Koch, M.; Darvill, N.; Scull, N.; Escalera-Maurer, A.; Sefer, L.; Wenman, R.; Lambert, S.; Jean, J.; Xu, Y.; Turner, B.; Kazarian, S. G.; Chapman, M. R.; Bubeck, D.; de Simone, A.; Knowles, T. P.; Matthews, S. J. Electrostatically-guided inhibition of Curli amyloid nucleation by the CsgC-like family of chaperones. *Sci. Rep.* **2016**, *6*, 24656.
(30) Chorell, E.; Andersson, E.; Evans, M. L.; Jain, N.; Götheson, A.; Åden, J.; Chapman, M. R.; Almqvist, F.; Wittung-Stafshede, P. Bacterial Chaperones CsgE and CsgC Differentially Modulate Human alpha-Synuclein Amyloid Formation via Transient Contacts. *PLoS One* **2015**, *10*, No. e0140194.
(31) Stenvang, M.; Dueholm, M. S.; Vad, B. S.; Seviour, T.; Zeng, G.; Geifman-Shochat, S.; Søndergaard, M. T.; Christiansen, G.; Meyer, R. L.; Kjelleberg, S.; Nielsen, P. H.; Otzen, D. E. Epigallocatechin Gallate Remodels Overexpressed Functional Amyloids in Pseudomonas aeruginosa and Increases Biofilm Susceptibility to Antibiotic Treatment. *J. Biol. Chem.* **2016**, *291*, 26540−26553.
(32) Ehrnhoefer, D. E.; Bieschke, J.; Boeddrich, A.; Herbst, M.; Masino, L.; Lurz, R.; Engemann, S.; Pastore, A.; Wanker, E. E. EGCG redirects amyloidogenic polypeptides into unstructured, off-pathway oligomers. *Nat. Struct. Mol. Biol.* **2008**, *15*, 558−566.
(33) Lorenzen, N.; Nielsen, S. B.; Yoshimura, Y.; Vad, B. S.; Andersen, C. B.; Betzer, C.; Kaspersen, J. D.; Christiansen, G.; Pedersen, J. S.; Jensen, P. H.; Mulder, F. A. A.; Otzen, D. E. How epigallocatechin gallate can inhibit alpha-synuclein oligomer toxicity in vitro. *J. Biol. Chem.* **2014**, *289*, 21299−21310.
(34) Andersson, E. K.; Bengtsson, C.; Evans, M. L.; Chorell, E.; Sellstedt, M.; Lindgren, A. E. G.; Hufnagel, D. A.; Bhattacharya, M.; Tessier, P. M.; Wittung-Stafshede, P.; Almqvist, F.; Chapman, M. R. Modulation of curli assembly and pellicle biofilm formation by chemical and protein chaperones. *Chem. Biol.* **2013**, *20*, 1245−1254.
(35) Nenninger, A. A.; Robinson, L. S.; Hammer, N. D.; Epstein, E. A.; Badtke, M. P.; Hultgren, S. J.; Chapman, M. R. CsgE is a curli secretion specificity factor that prevents amyloid fibre aggregation. *Mol. Microbiol.* **2011**, *81*, 486−499.
(36) Cegelski, L.; Pinkner, J. S.; Hammer, N. D.; Cusumano, C. K.; Hung, C. S.; Chorell, E.; Åberg, V.; Walker, J. N.; Seed, P. C.; Almqvist, F.; Chapman, M. R.; Hultgren, S. J. Small-molecule inhibitors target Escherichia coli amyloid biogenesis and biofilm formation. *Nat. Chem. Biol.* **2009**, *5*, 913−919.
(37) Horvath, I.; Weise, C. F.; Andersson, E. K.; Chorell, E.; Sellstedt, M.; Bengtsson, C.; Olofsson, A.; Hultgren, S. J.; Chapman, M.; Wolf-Watz, M.; Almqvist, F.; Wittung-Stafshede, P. Mechanisms of protein oligomerization: inhibitor of functional amyloids templates alpha-synuclein fibrillation. *J. Am. Chem. Soc.* **2012**, *134*, 3439−3444.
(38) Giehm, L.; Otzen, D. E. Experimental approaches to inducing amyloid. In *Amyloid Fibrils and Prefibrillar Aggregates*; Otzen, D. E., Ed.; Wiley-VCH Verlag GmbH, 2012; pp 295−320.
(39) van der Lee, R.; Buljan, M.; Lang, B.; Weatheritt, R. J.; Daughdrill, G. W.; Dunker, A. K.; Fuxreiter, M.; Gough, J.; Gsponer, J.; Jones, D. T.; Kim, P. M.; Kriwacki, R. W.; Oldfield, C. J.; Pappu, R. V.; Tompa, P.; Uversky, V. N.; Wright, P. E.; Babu, M. M. Classification of intrinsically disordered regions and proteins. *Chem. Rev.* **2014**, *114*, 6589−6631.
(40) Braak, H.; Tredici, K. D.; Rüb, U.; de Vos, R. A. I.; Jansen Steur, E. N. H.; Braak, E. Staging of brain pathology related to sporadic Parkinson's disease. *Neurobiol. Aging* **2003**, *24*, 197−211.
(41) Chen, H.; Zhao, E. J.; Zhang, W.; Lu, Y.; Liu, R.; Huang, X.; Ciesielski-Jones, A. J.; Justice, M. A.; Cousins, D. S.; Peddada, S. Meta-analyses on prevalence of selected Parkinson's nonmotor symptoms before and after diagnosis. *Transl. Neurodegener.* **2015**, *4*, 1.
(42) Wakabayashi, K.; Takahashi, H.; Takeda, S.; Ohama, E.; Ikuta, F. Parkinson's disease: the presence of Lewy bodies in Auerbach's and Meissner's plexuses. *Acta Neuropathol.* **1988**, *76*, 217−221.
(43) Braak, H.; de Vos, R. A. I.; Bohl, J.; Del Tredici, K. Gastric alpha-synuclein immunoreactive inclusions in Meissner's and Auerbach's plexuses in cases staged for Parkinson's disease-related brain pathology. *Neurosci. Lett.* **2006**, *396*, 67−72.
(44) Stokholm, M. G.; Danielsen, E. H.; Hamilton-Dutoit, S. J.; Borghammer, P. Pathological alpha-synuclein in gastrointestinal tissues from prodromal Parkinson disease patients. *Ann. Neurol.* **2016**, *79*, 940−949.
(45) Hilton, D.; Stephens, M.; Kirk, L.; Edwards, P.; Potter, R.; Zajicek, J.; Broughton, E.; Hagan, H.; Carroll, C. Accumulation of alpha-synuclein in the bowel of patients in the pre-clinical phase of Parkinson's disease. *Acta Neuropathol.* **2013**, *127*, 235−241.
(46) Killinger, B. A.; Madaj, Z.; Sikora, J. W.; Rey, N.; Haas, A. J.; Vepa, Y.; Lindqvist, D.; Chen, H.; Thomas, P. M.; Brundin, P.; Brundin, L.; Labrie, V. The vermiform appendix impacts the risk of developing Parkinson's disease. *Sci. Transl. Med.* **2018**, *10*, No. eaar5280.
(47) Holmqvist, S.; Chutna, O.; Bousset, L.; Aldrin-Kirk, P.; Li, W.; Björklund, T.; Wang, Z.-Y.; Roybon, L.; Melki, R.; Li, J.-Y. Direct evidence of Parkinson pathology spread from the gastrointestinal tract to the brain in rats. *Acta Neuropathol.* **2014**, *128*, 805−820.
(48) Uemura, N.; Yagi, H.; Uemura, M. T.; Hatanaka, Y.; Yamakado, H.; Takahashi, R. Inoculation of alpha-synuclein preformed fibrils into the mouse gastrointestinal tract induces Lewy body-like aggregates in the brainstem via the vagus nerve. *Mol. Neurodegener.* **2018**, *13*, 21.
(49) Furness, J. B.; Callaghan, B. P.; Rivera, L. R.; Cho, H.-J. The enteric nervous system and gastrointestinal innervation: integrated local and central control. *Adv. Exp. Med. Biol.* **2014**, *817*, 39−71.
(50) Bohórquez, D. V.; Shahid, R. A.; Erdmann, A.; Kreger, A. M.; Wang, Y.; Calakos, N.; Wang, F.; Liddle, R. A. Neuroepithelial circuit formed by innervation of sensory enteroendocrine cells. *J. Clin. Invest.* **2015**, *125*, 782−786.
(51) Bogunovic, M.; Davé, S. H.; Tilstra, J. S.; Chang, D. T. W.; Harpaz, N.; Xiong, H.; Mayer, L. F.; Plevy, S. E. Enteroendocrine cells express functional Toll-like receptors. *Am. J. Physiol.: Gastrointest. Liver Physiol.* **2007**, *292*, G1770−G1783.
(52) Tükel, Ç.; Nishimori, J. H.; Wilson, R. P.; Winter, M. G.; Keestra, A. M.; Van Putten, J. P. M.; Bäumler, A. J. Toll-like receptors

DOI: 10.1021/acsomega.8b03590
ACS Omega 2019, 4, 4029−4039

1 and 2 cooperatively mediate immune responses to curli, a common amyloid from enterobacterial biofilms. *Cell. Microbiol.* **2010**, *12*, 1495−1505.
(53) Rapsinski, G. J.; Wynosky-Dolfi, M. A.; Oppong, G. O.; Tursi, S. A.; Wilson, R. P.; Brodsky, I. E.; Tükel, Ç. Toll-like receptor 2 and NLRP3 cooperate to recognize a functional bacterial amyloid, curli. *Infect. Immun.* **2014**, *83*, 693−701.
(54) Kelly, L. P.; Carvey, P. M.; Keshavarzian, A.; Shannon, K. M.; Shaikh, M.; Bakay, R. A. E.; Kordower, J. H. Progression of intestinal permeability changes and alpha-synuclein expression in a mouse model of Parkinson's disease. *Mov. Disord.* **2013**, *29*, 999−1009.
(55) Forsyth, C. B.; Shannon, K. M.; Kordower, J. H.; Voigt, R. M.; Shaikh, M.; Jaglin, J. A.; Estes, J. D.; Dodiya, H. B.; Keshavarzian, A. Increased intestinal permeability correlates with sigmoid mucosa alpha-synuclein staining and endotoxin exposure markers in early Parkinson's disease. *PLoS One* **2011**, *6*, No. e28032.
(56) Sampson, T. R.; Debelius, J. W.; Thron, T.; Janssen, S.; Shastri, G. G.; Ilhan, Z. E.; Challis, C.; Schretter, C. E.; Rocha, S.; Gradinaru, V.; Chesselet, M.-F.; Keshavarzian, A.; Shannon, K. M.; Krajmalnik-Brown, R.; Wittung-Stafshede, P.; Knight, R.; Mazmanian, S. K. Gut Microbiota Regulate Motor Deficits and Neuroinflammation in a Model of Parkinson's Disease. *Cell* **2016**, *167*, 1469−1480.
(57) Chen, S. G.; Stribinskis, V.; Rane, M. J.; Demuth, D. R.; Gozal, E.; Roberts, A. M.; Jagadapillai, R.; Liu, R.; Choe, K.; Shivakumar, B.; Son, F.; Jin, S.; Kerber, R.; Adame, A.; Masliah, E.; Friedland, R. P. Exposure to the Functional Bacterial Amyloid Protein Curli Enhances Alpha-Synuclein Aggregation in Aged Fischer 344 Rats and Caenorhabditis elegans. *Sci. Rep.* **2016**, *6*, 34477.
(58) Monstein, H.-J.; Kraft, C. H.; Borch, K.; Tiveljung, A.; Jonasson, J. Profiling of bacterial flora in gastric biopsies from patients with Helicobacter pylori-associated gastritis and histologically normal control individuals by temperature gradient gel electrophoresis and 16S rDNA sequence analysis. *J. Med. Microbiol.* **2000**, *49*, 817−822.
(59) Studier, F. W. Protein production by auto-induction in high-density shaking cultures. *Protein Expression Purif.* **2005**, *41*, 207−234.
(60) Lorenzen, N.; Nielsen, S. B.; Buell, A. K.; Kaspersen, J. D.; Arosio, P.; Vad, B. S.; Paslawski, W.; Christiansen, G.; Valnickova-Hansen, Z.; Andreasen, M.; Enghild, J. J.; Pedersen, J. S.; Dobson, C. M.; Knowles, T. P. J.; Otzen, D. E. The Role of Stable α-Synuclein Oligomers in the Molecular Events Underlying Amyloid Formation. *J. Am. Chem. Soc.* **2014**, *136*, 3859−3868.
(61) Paslawski, W.; Lorenzen, N.; Otzen, D. E. Formation and Characterization of α-Synuclein Oligomers. *Methods Mol. Biol.* **2016**, *1345*, 133−150.
(62) Stochaj, W. R.; Berkelman, T.; Laird, N., Staining membrane-bound proteins with ponceau s. *CSH Protoc.* **2006**, *2006* (). DOI: 10.1101/pdb.prot4543
(63) Kim, J.-Y.; Sahu, S.; Yau, Y.-H.; Wang, X.; Shochat, S. G.; Nielsen, P. H.; Dueholm, M. S.; Otzen, D. E.; Lee, J.; Delos Santos, M. M. S.; Yam, J. K. H.; Kang, N.-Y.; Park, S.-J.; Kwon, H.; Seviour, T.; Yang, L.; Givskov, M.; Chang, Y.-T. Detection of Pathogenic Biofilms with Bacterial Amyloid Targeting Fluorescent Probe, CDy11. *J. Am. Chem. Soc.* **2016**, *138*, 402−407.
(64) Moran, S. D.; Zanni, M. T. How to Get Insight into Amyloid Structure and Formation from Infrared Spectroscopy. *J. Phys. Chem. Lett.* **2014**, *5*, 1984−1993.
(65) Danielsen, H. N.; Hansen, S. H.; Herbst, F. A.; Kjeldal, H.; Stensballe, A.; Nielsen, P. H.; Dueholm, M. S. Direct Identification of Functional Amyloid Proteins by Label-Free Quantitative Mass Spectrometry. *Biomolecules* **2017**, *7*, 58.
(66) Keshavarzian, A.; Green, S. J.; Engen, P. A.; Voigt, R. M.; Naqib, A.; Forsyth, C. B.; Mutlu, E.; Shannon, K. M. Colonic bacterial composition in Parkinson's disease. *Mov. Disord.* **2015**, *30*, 1351−1360.
(67) Greenwald, J.; Riek, R. Biology of amyloid: structure, function, and regulation. *Structure* **2010**, *18*, 1244−1260.
(68) Collinson, S. K.; Parker, J. M. R.; Hodges, R. S.; Kay, W. W. Structural predictions of AgfA, the insoluble fimbrial subunit of Salmonella thin aggregative fimbriae. *J. Mol. Biol.* **1999**, *290*, 741−756.
(69) Toombs, J. A.; McCarty, B. R.; Ross, E. D. Compositional determinants of prion formation in yeast. *Mol. Cell. Biol.* **2009**, *30*, 319−332.
(70) Hinman, M. B.; Lewis, R. V. Isolation of a clone encoding a second dragline silk fibroin. Nephila clavipes dragline silk is a two-protein fiber. *J. Biol. Chem.* **1992**, *267*, 19320−19324.
(71) Liu, L.; Murphy, R. M. Kinetics of Inhibition of β-Amyloid Aggregation by Transthyretin. *Biochemistry* **2006**, *45*, 15702−15709.
(72) Jain, N.; Ådén, J.; Nagamatsu, K.; Evans, M. L.; Li, X.; McMichael, B.; Ivanova, M. I.; Almqvist, F.; Buxbaum, J. N.; Chapman, M. R. Inhibition of curli assembly and Escherichia coli biofilm formation by the human systemic amyloid precursor transthyretin. *Proc. Natl. Acad. Sci. U.S.A.* **2017**, *114*, 12184−12189.
(73) Goedert, M.; Jakes, R.; Spillantini, M. G.; Hasegawa, M.; Smith, M. J.; Crowther, R. A. Assembly of microtubule-associated protein tau into Alzheimer-like filaments induced by sulphated glycosaminoglycans. *Nature* **1996**, *383*, 550−553.
(74) Giasson, B. I.; Forman, M. S.; Higuchi, M.; Golbe, L. I.; Graves, C. L.; Kotzbauer, P. T.; Trojanowski, J. Q.; Lee, V. M. Initiation and synergistic fibrillization of tau and alpha-synuclein. *Science* **2003**, *300*, 636−640.

DOI: 10.1021/acsomega.8b03590
ACS Omega 2019, 4, 4029−4039